Taylor & Francis
Taylor & Francis Group

Combustion Science and Technology

ISSN: 0010-2202 (Print) 1563-521X (Online) Journal homepage: http://www.tandfonline.com/loi/gcst20

Simplified Reaction Mechanisms for the Oxidation of Hydrocarbon Fuels in Flames

CHARLES K. WESTBROOK & FREDERICK L DRYER

To cite this article: CHARLES K. WESTBROOK & FREDERICK L DRYER (1981) Simplified Reaction Mechanisms for the Oxidation of Hydrocarbon Fuels in Flames, Combustion Science and Technology, 27:1-2, 31-43, DOI: 10.1080/00102208108946970

To link to this article: http://dx.doi.org/10.1080/00102208108946970

Combustion Science and Technology, 1981, Vol. 27, pp. 31–43
0010-2202/81/2702-0031$06.50/0

Simplified Reaction Mechanisms for the Oxidation of Hydrocarbon Fuels in Flames

CHARLES K. WESTBROOK *Lawrence Livermore National Laboratory, Livermore CA 94550*

FREDERICK L. DRYER *Department of Mechanical and Aerospace Engineering, Princeton University, Princeton, NJ 08544*

(*Received December 22, 1980; in final form July 6, 1981*)

Abstract—Simplified reaction mechanisms for the oxidation of hydrocarbon fuels have been examined using a numerical laminar flame model. The types of mechanisms studied include one and two global reaction steps as well as quasi-global mechanisms. Reaction rate parameters were varied in order to provide the best agreement between computed and experimentally observed flame speeds in selected mixtures of fuel and air. The influences of the various reaction rate parameters on the laminar flame properties have been identified, and a simple procedure to determine the best values for the reaction rate parameters is demonstrated. Fuels studied include *n*-paraffins from methane to *n*-decane, some methyl-substituted *n*-paraffins, acetylene, and representative olefin, alcohol and aromatic hydrocarbons. Results show that the often-employed choice of simultaneous first order fuel and oxidizer dependence for global rate expressions cannot yield the correct dependence of flame speed on equivalence ratio or pressure and cannot correctly predict the rich flammability limit. However, the best choice of rate parameters suitably reproduces rich and lean flammability limits as well as the dependence of the flame speed on pressure and equivalence ratio for all of the fuels examined. Two-step and quasi-global approaches also yield information on flame temperature and burned gas composition. However, none of the simplified mechanisms studied accurately describes the chemical structure of the flame itself.

INTRODUCTION

Flame propagation is a central problem in most practical combustion systems. Recent theoretical flame models (Smoot *et al.*, 1976; Tsatsaronis, 1978; Westbrook and Dryer, 1980a) have emphasized the importance of detailed chemical kinetics in these problems and have provided significant new insights into the structure of flames. However, there is a continuing need for reliable models for fuel oxidation which are very simple and yet still reproduce experimental flame propagation phenomena over extended ranges of operating conditions.

For example, numerical models of combustors which consider two- or three-dimensional geometry cannot currently include detailed kinetic mechanisms because the computational costs of such a treatment would be much too great. In addition, detailed mechanisms have been developed and validated only for the simplest fuel molecules (Westbrook and Dryer, 1980b) and are not available for most practical fuels. Finally, there are many occasions where the great amount of chemical information produced by a detailed reaction mechanism is not necessary and a simple mechanism will suffice.

The use of simplified reaction mechanisms in describing flame properties for hydrocarbon–air mixtures can be traced to the work of Zeldovich and Frank-Kamenetsky (1938) and Semenov (1942). These early formulations were concerned primarily with the prediction of *quasi-steady-state* laminar flame speeds, and some very significant achievements using them were reported (*e.g.* Simon, 1951; Walker and Wright, 1952). In recent years, however, many combustion problems have arisen that require a *time-dependent* kinetics formulation which can be coupled with a fluid mechanics model to predict and evaluate overall system performance.

Any simplified reaction mechanism which is used must be capable of reproducing experimental flame properties over the range of operating conditions under consideration. As we will demonstrate, many of the simple kinetics models in common use do not satisfy this requirement and can give erroneous results. In this paper we review some of the properties of simple reaction mechanisms and provide recommendations concerning their use in modeling flame propagation.

We will begin by examining some of the characteristics of laminar flame propagation, using a single-

step global rate expression. We will then discuss refinements in the reaction mechanism which are accomplished by breaking the global reaction into two or more partial steps.

All of the flame model computations described in this paper have been carried out using the HCT code of Lund (1978). This same code has been used in our previous studies of flame propagation using detailed chemical kinetic reaction mechanisms, with the only difference here being that simplified reaction mechanisms have been used. The model solves one-dimensional finite difference equations for conservation of mass, momentum, energy, and each chemical species. A moving grid system enables additional spatial zones to be concentrated in the flame region. The model is fully time-dependent so the steady-state propagation of a flame is treated as the time-asymptotic solution of an unsteady problem. Each flame model described here required 1–2 minutes of time on a CDC 7600 computer. Transport coefficients, including thermal diffusivity and molecular species diffusivities, have been taken directly from our previous studies of laminar flame propagation using detailed kinetics. In this simplified formulation, the thermal diffusivity D_T and the molecular diffusivity D_i for species i are represented by functional forms

$$D_T = a_0 T^{1/2}/C_{tot}$$

$$D_i = a_1 T^{1/2}/(C_{tot} W_i)$$

where C_{tot} is the total species concentration and W_i is the molecular weight of species i. The coefficients a_0 and a_1 were determined by requiring that the numerical model, with a detailed chemical kinetics reaction mechanism, correctly reproduce the experimentally measured flame speed for stoichiometric methane–air and methanol–air mixtures (Westbrook and Dryer, 1979). The values for a_0 and a_1 are 1.92×10^{-6} and 9.26×10^{-6} respectively. In simplified mechanisms most species are omitted, particularly the highly diffusive radical species such as H, O, and OH. As a result, features of the flame structure which depend on details of the molecular species transport cannot be resolved by these mechanisms regardless of the model chosen for the diffusivities.

SINGLE-STEP REACTION MECHANISMS

The simplest overall reaction representing the oxidation of a conventional hydrocarbon fuel is

$$\text{Fuel} + n_1 O_2 \rightarrow n_2 CO_2 + n_3 H_2O \qquad (1)$$

where $\{n_i\}$ are determined by the choice of fuel. This global reaction is often a convenient way of approximating the effects of the many elementary reactions which actually occur. Its rate must therefore represent an appropriate average of all of the individual reaction rates involved. The rate expression of the single reaction is usually expressed

$$k_{ov} = AT^n \exp(-E_a/RT)[\text{Fuel}]^a[\text{Oxidizer}]^b. \qquad (2)$$

In this paper we consider only hydrocarbon fuels and assume the oxidizer to be molecular oxygen, although the treatment described below can be applied to other types of fuels and/or oxidizers.

We can illustrate many of the features of the use of global rate expressions for laminar flame propagation for the case of n-octane (C_8H_{18}) in air. The experimental flammability limits are $\phi_L' = 0.5$ and $\phi_R' = 4.3$, and the maximum flame speed is approximately 42 cm/sec at $\phi \simeq 1.15$ (Dugger *et al.*, 1959). For stoichiometric mixtures, the laminar flame speed S_u is approximately 40 cm/sec.

With the transport coefficients predetermined by our previous work, only the rate expression, Eq. (2), can be adjusted to provide agreement between computed and experimental results. For convenience we have assumed $n = 0$ in Eq. (2), while for the effective activation energy E_a we have used 30 kcal/mole as an appropriate average between the lower values ($\sim$26 kcal/mole) determined by Fenn and Calcote (1952) and the higher value (40 kcal/mole) used by Walker and Wright. We will show below that variation of E_a over the range 26–40 kcal/mole affects only the computed flame thickness, and results obtained with $E_a = 30$ kcal/mole were quite satisfactory.

A simple procedure was followed to evaluate the remaining parameters in the overall rate expression. Values were assumed for the concentration exponents a and b. Then with n set to zero and E_a, a, and b held fixed, the pre-exponential A was varied until the model correctly predicted the flame speed for an atmospheric pressure, stoichiometric fuel–air mixture, *e.g.* 40 cm/sec for C_8H_{18}. The resulting rate expression was then used to predict flame speeds for fuel–air mixtures at other equivalence ratios and pressures. Each set of rate expression parameters was then evaluated on the basis of how well it reproduced experimental data, relative to the one calibration point at $\phi = 1.0$ and atmospheric pressure.

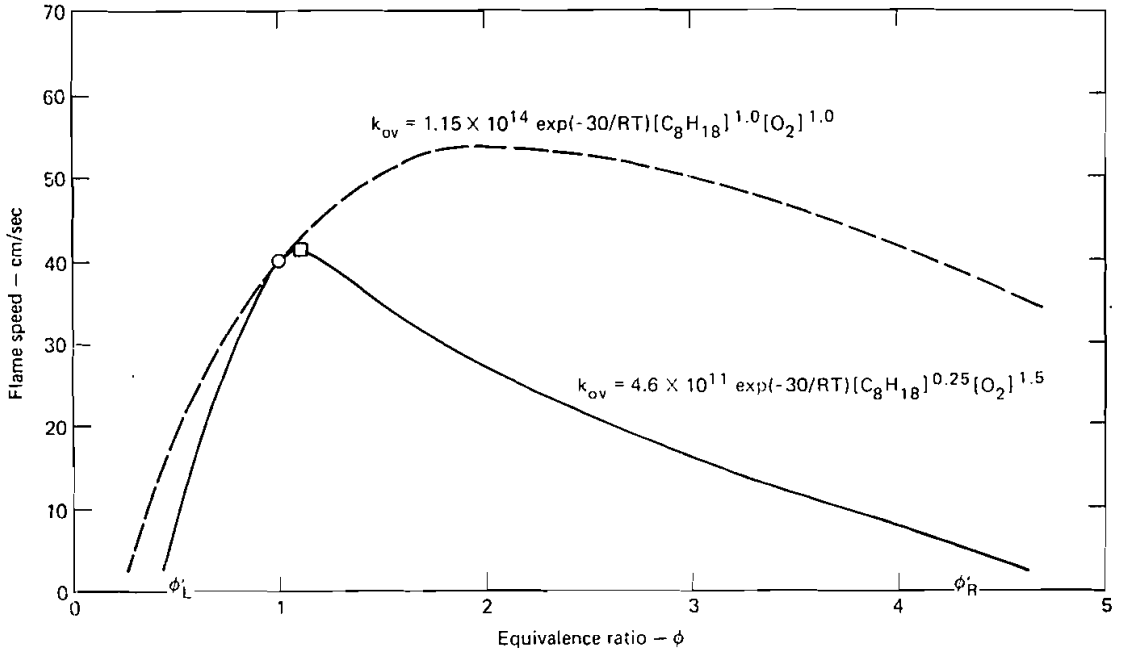

FIGURE 1 Variation of flame speed with equivalence ratio for *n*-octane in air, computed using the single-step reaction rates indicated. Experimental values for the lean and rich flammability limits ($\phi_L'=0.5$ and $\phi_R'=4.3$) for the observed flame speed at $\phi=1$ (open circle), and for the maximum flame speed (open square) are also indicated.

The most common assumption in the combustion literature for the concentration exponents is that the rate expression is first order in both fuel and oxidizer, *i.e.* $a=b=1$. Following the procedure outlined above, the resulting rate expression is

$$k_{ov}=1.15\times10^{14}\exp(-30/RT)[C_8H_{18}]^{1.0}[O_2]^{1.0} \quad (3)$$

which correctly predicts a flame speed of 40 cm/sec for $\phi=1$ and atmospheric pressure. Predicted flame speed as a function of equivalence ratio is plotted in Figure 1, together with the experimental data. It is clear that this rate expression does not reproduce the experimental flame speed curve. In particular computed flame speeds for fuel-rich mixtures are much too high, and an extrapolation of the curve gives a rich flammability limit ϕ_R of approximately 10. The maximum flame speed of nearly 55 cm/sec occurs near $\phi=2$, again in considerable disagreement with experimental results.

These computed results show that the assumption of a reaction rate expression that is first order in both fuel and oxidizer concentrations leads to serious errors in computed flame speeds, particularly for rich mixtures. Only for the special case of a stoichiometric fuel–air mixture, for which the rate parameters were evaluated, does Eq. (3) predict the proper flame speed. The inadequacy of the assumption of $a=b=1$ was observed for all of the hydrocarbon fuels examined in this study. As a result, we conclude that this rate expression should not be used in models for any combustion problems in which the fuel–air equivalence ratio varies with time or position.

It was found that significant improvements in predicted flame speeds could be obtained with different choices for the concentration exponents a and b. The flame speed depends strongly on the fuel concentration exponent a for rich mixtures and on the oxygen concentration exponent b for lean mixtures. The best agreement between computed and experimental results was obtained with

$$k_{ov}=4.6\times10^{11}\exp(-30/RT)[C_8H_{18}]^{0.25}[O_2]^{1.5}. \quad (4)$$

The computed results with this rate expression are also shown in Figure 1. The computed flammability limits are $\phi_L\approx0.5$ and $\phi_R\approx4.5$, and the maximum

flame speed of about 42 cm/sec occurs slightly on the rich side of stoichiometric, all in good agreement with experiment.

For large hydrocarbon fuel molecules like *n*-octane, an increase in equivalence ratio from $\phi = 1$ to $\phi = 2$ increases the fuel concentration by about 100 percent while the O_2 concentration decreases by less than 2 percent. Therefore, Eq. (3) predicts that the reaction rate is roughly proportional to ϕ over the range ($1 < \phi < 10$). This rapid increase more than compensates for the gradual decrease in flame temperature and leads to the observed overestimate of the reaction rate when $a = b = 1$. The concentration exponents in Eq. (4) correct this.

Simple flame theory predicts that the flame speed is approximately proportional to the square root of the reaction rate. One can substitute the unburned fuel and oxygen concentrations into Eq. (3) or Eq. (4), together with an appropriate temperature, to estimate the flame speed for a specified set of fuel–air mixtures. If that temperature were independent of the equivalence ratio or equal to the adiabatic flame temperature, then it would be simple to predict flammability limits and maximum flame speed for a given fuel from thermodynamic data alone, without having to carry out the computations described here with a full flame model. However, we found that neither the adiabatic flame temperature nor any constant temperature; combined with the concentrations in Eq. (3) or Eq. (4), provided a reliable estimate of the dependence of flame speed on equivalence ratio. In particular, the adiabatic flame temperature for rich mixtures falls too rapidly with increasing equivalence ratio, leading to a substantial underestimate of the rich flammability limit. At the other extreme, the use of a constant temperature ($T = 1500$ K) leads to an overestimate for the rich limit, about $\phi = 30$ for the case of *n*-octane.

In the computed flame models the rate of heat release due to chemical reactions varies through the flame, reaching a maximum near the point at which the spatial temperature gradient attains its maximum value. The temperature in the flame zone at the point where the heat release rate is a maximum, used in Eq. (3) or Eq. (4), was found to provide a good estimate of the dependence of flame speed on equivalence ratio. However, it is necessary to carry out the full flame model calculation to determine that temperature, which varies with equivalence ratio from 1450 K to approximately 2000 K. We were unable to derive an analytic or thermodynamic method of determining, *a priori*, the variation in flame speed due to changes in fuel or oxigen concentrations. For each fuel examined, the actual flame models provided the only reliable value for the flame speed.

Another important consideration in many combustion applications is the variation of flame speed with pressure. For most hydrocarbon–air mixtures the flame speed decreases with increasing pressure. Often this can be expressed in the form

$$S_u = S_0 P^{-x} \tag{5}$$

where S_0 and x are constants which depend on the choice of fuel. Detailed kinetic modeling studies of methane–air (Tsatsaronis, 1978; Westbrook and Dryer, 1980a) and methanol–air (Westbrook and Dryer, 1980a) mixtures have shown that the pressure exponent x has a very small value for low pressure conditions ($P \leqslant 1$ atm) and a larger value for higher pressures ($P \geqslant 4$ atm), with a transitional region between these ranges. In our own modeling study we showed that this behavior is primarily due to the effects of radical recombination reactions, particularly $H + O_2 + M = HO_2 + M$, which becomes important above atmospheric pressure, competing with chain branching reactions. With respect to global reaction modeling, these conclusions mean that it is not possible to reproduce both the higher and lower pressure range with a single rate expression in Eq. (4). We could not find experimental data on the dependence of flame speed on pressure for *n*-octane at elevated pressures, but data for propane–air (Metghalchi and Keck, 1980), and for methanol–air and isooctane–air (Metghalchi and Keck, 1977) have been obtained, and numerical predictions for methanol–air have also appeared (Westbrook and Dryer, 1980a). These results for pressures in the range of 1–25 atm yield a pressure exponent between -0.10 and -0.20 for stoichiometric fuel–air mixtures. The rate expression in Eq. (4) predicts flame speeds for *n*-octane–air which vary approximately as $P^{-0.12}$, consistent with available data for other fuels. For a simplified global kinetics model the pressure dependence of the flame speed can be shown (Adamczyk and Lavoie, 1978) to be approximately

$$S_u \propto P^{(a+b-2)/2} \tag{6}$$

For the rate expression in Eq. (4) this gives $P^{-0.125}$, again consistent with the computed results. In order to reproduce the pressure dependence of flame speed at low pressure ($P \leqslant 1$ atm), the oxygen concentration exponent must be set equal to approximately

TABLE I

Single-step reaction rate parameters giving best agreement between experimental flammability limits (ϕ_L' and ϕ_R') and computed flammability limits (ϕ_L and ϕ_R). Units are cm-sec-mole-kcal-Kelvins

Fuel	A	E_a	a	b	ϕ_L'	ϕ_L	ϕ_R'	ϕ_R
CH_4	1.3×10^8	48.4	−0.3	1.3	0.5	0.5	1.6	1.6
CH_4	8.3×10^5	30.0	−0.3	1.3	0.5	0.5	1.6	1.6
C_2H_6	1.1×10^{12}	30.0	0.1	1.65	0.5	0.5	2.7	3.1
C_3H_8	8.6×10^{11}	30.0	0.1	1.65	0.5	0.5	2.8	3.2
C_4H_{10}	7.4×10^{11}	30.0	0.15	1.6	0.5	0.5	3.3	3.4
C_5H_{12}	6.4×10^{11}	30.0	0.25	1.5	0.5	0.5	3.6	3.7
C_6H_{14}	5.7×10^{11}	30.0	0.25	1.5	0.5	0.5	4.0	4.1
C_7H_{16}	5.1×10^{11}	30.0	0.25	1.5	0.5	0.5	4.5	4.5
C_8H_{18}	4.6×10^{11}	30.0	0.25	1.5	0.5	0.5	4.3	4.5
C_8H_{18}	7.2×10^{12}	40.0	0.25	1.5	0.5	0.5	4.3	4.5
C_9H_{20}	4.2×10^{11}	30.0	0.25	1.5	0.5	0.5	4.3	4.5
$C_{10}H_{22}$	3.8×10^{11}	30.0	0.25	1.5	0.5	0.5	4.2	4.5
CH_3OH	3.2×10^{12}	30.0	0.25	1.5	0.5	0.5	4.1	4.0
C_2H_5OH	1.5×10^{12}	30.0	0.15	1.6	0.5	0.5	3.4	3.6
C_6H_6	2.0×10^{11}	30.0	−0.1	1.85	0.5	0.5	3.4	3.6
C_7H_8	1.6×10^{11}	30.0	−0.1	1.85	0.5	0.5	3.2	3.5
C_2H_4	2.0×10^{12}	30.0	0.1	1.65	0.4	0.4	6.7	6.5
C_3H_6	4.2×10^{11}	30.0	−0.1	1.85	0.5	0.5	2.8	3.0
C_2H_2	6.5×10^{12}	30.0	0.5	1.25	0.3	0.3	>10.0	>10.0

1.65, yielding a $P^{-0.05}$ dependence. Note that Eq. (6) predicts no variation of flame speed with pressure when $a=b=1$; computations using the parameters in Eq. (3) confirmed this prediction.

All of the previous calculations were carried out with $E_a=30$ kcal/mole. If a different value is used, then in principle one must redetermine a, b, and A, and then re-evaluate the resulting rate expression by comparison between computed and experimental flame speed data. In practice, the concentration exponents were found to be nearly independent of E_a, leaving A as the only parameter to be redetermined. With an effective activation energy of 40 kcal/mole, the rate expression becomes

$$k_{ov}=7.2\times10^{12}\exp(-40/RT)[C_8H_{18}]^{0.25}[O_2]^{1.5}. \quad (7)$$

Flames computed by means of Eq. (7) and those from Eq. (4) differed by about 15 percent in the computed flame thickness, with the higher value of E_a leading to a thinner flame. In the absence of experimental flame thickness data which could distinguish between the two calculations, we have chosen to use the value of $E_a=30$ kcal/mole for the activation energy.

The sensitivity of the computed flame speeds to the fuel concentration exponent in Eq. (2) has required that $a=0.25$. In addition, if $a+b=1.75$, then the global mechanism will also reproduce the desired pressure dependence of the flame speed for pressures greater than or equal to atmospheric. In principle the oxidizer concentration exponent b determines the lean flammability limit, leaving three conditions (ϕ_R, ϕ_L, and pressure exponent) to be satisfied by two constants a and b. Fortunately, computed results on the lean side of stoichiometric are rather insensitive to variations in the oxygen concentration exponent. Thus it is possible to satisfy all of the observed behaviour with one set of concentration exponents.

The same sequence of operations has been carried out for the n-paraffin hydrocarbon series through n-decane, as well as other selected fuels. In each case the agreement between the experimental flame speed data and the computed results was similar to that shown in Figure 1 for n-octane using Eq. (4). In every case, rate parameters with $a=b=1$ seriously overestimated flame speeds for rich mixtures and rich flammability limits. The parameters which were found to give the best results for each fuel are summarized in Table I. Also shown are the computed flammability limits and the experimental limits from Dugger *et al.* (1959) or Lewis and von Elbe (1961). Except for methane, the values of a and b have been selected to give a pressure dependence of $P^{-0.125}$. For each fuel, the use of a smaller

value for the fuel concentration exponent leads to a lower predicted value for the rich flammability limit. For *n*-decane, if $a=0.15$ and $b=1.6$, the predicted rich flammability limit is $\phi_R=3.6$. This demonstrates how the rate data in Table I can be modified in order to fit flammability limits which may be more reliable than those of Dugger *et al.* or Lewis and von Elbe, or for fuels not included in their tabulations.

The results for methane require further comment. Methane oxidation in most experimental regimes is atypical of *n*-paraffin fuels. The flame speed for $\phi=1$ and atmospheric pressure is less than that for the other fuels (~38 cm/sec). The flammability limits are considerably narrower, and the pressure dependence ($P^{-0.5}$) is greater. These considerations require a somewhat different set of rate parameters than for the other fuels. The pressure dependence $P^{-0.5}$ indicates that $a+b=1.0$, while the observed rich flammability limit of $\phi_R'=1.6$ requires $a=-0.3$. Fenn and Calcote found that the effective activation energy for methane oxidation at high temperatures was the same as for the other *n*-paraffin fuels examined, leading to the use of 30 kcal/mole in one series of calculations. However, methane oxidation in shock tubes (Heffington *et al.*, 1976) and in the turbulent flow reactor (Dryer and Glassman, 1972) is characterized by a considerably higher overall activation energy of about 48.4 kcal/mole, so this value was also used. In both cases the best concentration exponents were found to be the same. The flame thickness in the model with $E_a=30$ kcal/mole was about 30 percent greater than when $E_a=48.4$ kcal/mole, but the flame speeds and their dependence on pressure and equivalence ratio were essentially the same for both models.

The fuel concentration exponent for CH_4 from Table I has a negative value, -0.3. Technically, the fuel acts as an inhibitor, similar to observations for methane ignition in shock tubes (*e.g.* Bowman, 1970). From a numerical point of view this can create problems since the rate of methane consumption increases without limit as the methane concentration approaches zero. There are several possible solutions to this problem. A reverse reaction can be used which provides an equilibrium fuel concentration at some small level, preventing the rate expression from becoming too large. The rate expression can also be artificially truncated at some predetermined value. However, in some cases it may be preferable to sacrifice some of the generality provided by the rate parameters in Table I in order to keep the rate expression conveniently bounded. Specifically, it is possible to reproduce the flame speed dependence on equivalence ratio at a given pressure with concentration exponents which do not satisfy the constraint $a+b=1.0$ and therefore will not reproduce the correct dependence of flame speed on pressure. Several rate expressions of this type were tested. The parameter sets are summarized in Table II and the results are shown in Figure 2. For methane–air mixtures at atmospheric pressure, flame speeds computed using a detailed reaction mechanism (Westbrook and Dryer, 1980a) agree well with experimental data (Andrews and Bradley, 1972; Garforth and Rallis, 1978) and are indicated by the solid curve in Figure 2. The computed flame speed using the parameters from Table I provide the closest agreement with the experimental data, but

TABLE II

Single-step and detailed reaction rate parameters for methane–air, corresponding to curves in Figure 2. Same units as Table I

	A	E_a	a	b
Set 1	Detailed reaction mechanism			
Set 2	1.3×10^{8}	48.4	−0.3	1.3
Set 3	6.7×10^{12}	48.4	0.2	1.3
Set 4	1.0×10^{13}	48.4	0.7	0.8
Set 5	2.4×10^{16}	48.4	1.0	1.0

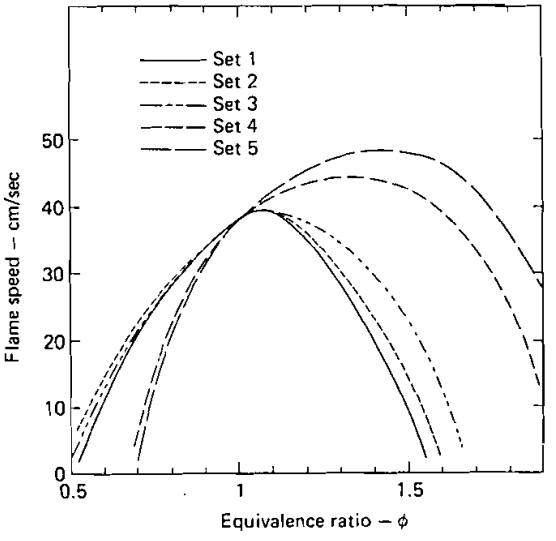

FIGURE 2 Variation of flame speed with equivalence ratio for methane in air, computed using the reaction mechanisms in Table II

TABLE III

Burned gas properties in methane–air mixtures, computed using detailed single-step and two-step reaction mechanisms

	Detailed mechanism			One-step mechanism	Two-step mechanism	
ϕ	T_{ad}	$[CO]/[CO_2]$	$[H_2]/[H_2O]$	T_{ad}	T_{ad}	$[CO]/[CO_2]$
0.8	1990	0.03	0.005	2017	1975	0.08
1.0	2220	0.11	0.02	2320	2250	0.14
1.2	2140	0.69	0.15	2260	2200	0.43

parameter Set 3, with $a=0.2$, $b=1.3$ also shows quite good agreement. Set 4, using concentration exponents taken from the dilute flow reactor experiments of Dryer and Glassman and Set 5, with $a=b=1.0$, both predict flame speeds in substantial disagreement with experimental values, especially for rich mixtures. Of the simplified mechanisms, only Set 2 predicts the proper variation of flame speed with pressure above one atmosphere.

TWO-STEP REACTION MECHANISMS

The single-step mechanism predicts flame speeds reliably over considerable ranges of conditions, but it has several flaws which can be important in certain applications. By assuming that the reaction products are CO_2 and H_2O, the total heat of reaction is overpredicted. At adiabatic flame temperatures typical of hydrocarbon fuels ($\sim$2000 K) substantial amounts of CO and H_2 exist in equilibrium in the combustion products with CO_2 and H_2O. The same is true to a lesser extent with other species, including some of the important free radical species such as H, O, and OH. This equilibrium lowers the total heat of reaction and the adiabatic flame temperature below the values predicted by Eq. (1). We can illustrate in Table III the magnitude of this effect in the case of methane–air mixtures, for which detailed reaction mechanisms exist, showing the predicted adiabatic flame temperatures from the detailed mechanism together with those obtained using the single-step model described earlier. Also shown are the burned-gas equilibrium ratios from the detailed model for $[CO]/[CO_2]$ and $[H_2]/[H_2O]$. The overestimate of adiabatic flame temperature by the single-step mechanism grows with increasing equivalence ratio and is directly related to the amounts of CO and H_2 in the reaction products.

In addition to the fact that the burned gas contains these incompletely oxidized species, it is also well recognized that typical hydrocarbons burn in a sequential manner. That is, the fuel is partially oxidized to CO and H_2, which are not appreciably consumed until all of the hydrocarbon species have disappeared (Dryer and Westbrook, 1979). Dryer and Glassman used this observation to construct a two-reaction model for methane oxidation in a turbulent flow reactor

$$\begin{aligned} CH_4 + 3/2O_2 &= CO + 2H_2O \\ CO + 1/2O_2 &= CO_2, \end{aligned} \tag{8}$$

with empirically derived rates for both reactions.

To account at least in part for the effects of incomplete conversion to CO_2 and H_2O, and to include qualitatively the sequential nature of the hydrocarbon oxidation, the reaction mechanism of Eq. (1) can be modified, following Dryer and Glassman, to include two steps. For example, with hydrocarbon fuels this results in

$$C_nH_m + \left(\frac{n}{2} + \frac{m}{4}\right)O_2 = nCO + \frac{m}{2}H_2O \tag{9a}$$

$$CO + 1/2O_2 = CO_2. \tag{9b}$$

The rate of the CO oxidation reaction has been taken from Dryer and Glassman and has the value

$$k_{9b} = 10^{14.6}\exp(-40/RT) \times [CO]^1[H_2O]^{0.5}[O_2]^{0.25} \tag{10}$$

In order to reproduce both the proper heat of reaction and pressure dependence of the $[CO]/[CO_2]$ equilibrium, a reverse reaction was defined for

TABLE IV

Parameters for two-step and quasi-global reaction mechanisms giving best agreement between experimental and computed flammability limits. Same units as Table I

	Two-step mechanism				Quasi-global mechanism			
Fuel	A	E_a	a	b	A	E_a	a	b
CH_4	2.8×10^{9}	48.4	−0.3	1.3	4.0×10^{9}	48.4	−0.3	1.3
CH_4	1.5×10^{7}	30.0	−0.3	1.3	2.3×10^{7}	30.0	−0.3	1.3
C_2H_6	1.3×10^{12}	30.0	0.1	1.65	2.0×10^{12}	30.0	0.1	1.65
C_3H_8	1.0×10^{12}	30.0	0.1	1.65	1.5×10^{12}	30.0	0.1	1.65
C_4H_{10}	8.8×10^{11}	30.0	0.15	1.6	1.3×10^{12}	30.0	0.15	1.6
C_5H_{12}	7.8×10^{11}	30.0	0.25	1.5	1.2×10^{12}	30.0	0.25	1.5
C_6H_{14}	7.0×10^{11}	30.0	0.25	1.5	1.1×10^{12}	30.0	0.25	1.5
C_7H_{16}	6.3×10^{11}	30.0	0.25	1.5	1.0×10^{12}	30.0	0.25	1.5
C_8H_{18}	5.7×10^{11}	30.0	0.25	1.5	9.4×10^{11}	30.0	0.25	1.5
C_8H_{18}	9.6×10^{12}	40.0	0.25	1.5	1.5×10^{13}	40.0	0.25	1.5
C_9H_{20}	5.2×10^{11}	30.0	0.25	1.5	8.8×10^{11}	30.0	0.25	1.5
$C_{10}H_{22}$	4.7×10^{11}	30.0	0.25	1.5	8.0×10^{11}	30.0	0.25	1.5
CH_3OH	3.7×10^{12}	30.0	0.25	1.5	7.3×10^{12}	30.0	0.25	1.5
C_2H_5OH	1.8×10^{12}	30.0	0.15	1.6	3.6×10^{12}	30.0	0.15	1.6
C_6H_6	2.4×10^{11}	30.0	−0.1	1.85	4.3×10^{11}	30.0	−0.1	1.85
C_7H_8	1.9×10^{11}	30.0	−0.1	1.85	3.4×10^{11}	30.0	−0.1	1.85
C_2H_4	2.4×10^{12}	30.0	0.1	1.65	4.3×10^{12}	30.0	0.1	1.65
C_3H_6	5.0×10^{11}	30.0	−0.1	1.85	8.0×10^{11}	30.0	−0.1	1.85
C_2H_2	7.8×10^{12}	30.0	0.5	1.25	1.2×10^{13}	30.0	0.5	1.25

Reaction 9b, with a rate

$$k_{-9b} = A\exp(-40/RT)[CO_2]^d. \qquad (11)$$

The concentration exponent d must be less than the sum of the exponents in Eq. (10) in order to allow the ratio $[CO]/[CO_2]$ to decrease with increasing pressure. Satisfactory results were obtained with $d=1$, $A=5\times10^{8}$.

The resulting two-reaction model was applied to the methane–air flames discussed earlier. The rate of Reaction 9a was assumed to have the form of Eq. (2), and the temperature exponent n was again set to zero. The best agreement between experimental and computed flame speeds was again obtained for $a=-0.3$, $b=1.3$ for both 30 kcal/mole and 48.4 kcal/mole activation energy. Only the pre-exponential A had to be adjusted to account for the differences occurring due to the use of Reaction 9b. In Table III the adiabatic flame temperature and computed ratio $[CO]/[CO_2]$ for the two-step mechanism is given for each equivalence ratio. From this data it is clear that the two-step mechanism provides a more accurate estimation of the flame parameters than the one-step mechanism. For methane–air and the other hydrocarbon–air flames, the two-step mechanism predicts flame speeds in close agreement with those predicted by the single-step model, over the same ranges of equivalence ratio and pressure. The addition of the CO–CO_2 equilibrium has improved the mechanism by providing a better adiabatic flame temperature and a reasonable estimate of the CO concentration at equilibrium. Further refinement in expressing the dissociation effects on burned gas temperature would lead to additional improvements. For each of the fuels examined, the reaction rate parameters which gave the best agreement with experimental data are summarized in Table IV.

MULTISTEP GLOBAL REACTION MECHANISMS

Another reaction can be added to account for the H_2–H_2O equilibrium in the burned gas region. For each reaction added another species equilibrium concentration can be estimated. The logical limit of this process is the quasi-global reaction mechanism of Edelman and Fortune (1969) which combines a single reaction of fuel and oxygen to form CO and H_2, together with a detailed reaction mechanism for CO and H_2 oxidation. Since all of the important elementary reactions and species in the CO–H_2–O_2

system can be included, this approach can provide accurate values for T_{ad} and the equilibrium post-flame composition. Because thermal NO_x production in flames depends primarily on burned gas properties, the extended Zeldovich mechanism reactions can be added to the quasi-global reactions to give an estimate of NO_x formation rates. Alternatively, algebraic equations for the chemical equilibrium in the post-flame gases can be used instead of the partial differential equations which must be solved in the quasi-global formulation. As we will show, radical levels in the flame zone itself are not predicted accurately by the quasi-global model (Dryer and Westbrook), so NO_x production due to radical overshoot will not be predicted correctly.

The computational costs of a given reaction mechanism depend primarily on the number of chemical species included, rather than on the number of reactions. Conventional numerical solution techniques for the differential equations encountered in both detailed and simplified kinetics schemes indicate that the computer time requirements are roughly proportional to N^2, where N is the number of species. For the single-step mechanism of Eq. (1) there are 5 species including nitrogen, and 6 species with Reactions 9a and 9b. Because of the N^2 dependence, each additional species increases the computer costs by a significant margin. The CO–H_2–O_2 mechanism includes 10–12 species (H, O, H_2, O_2, OH, H_2O, N_2, CO, CO_2, fuel and possibly HO_2 and H_2O_2), while detailed mechanisms for methane or methanol oxidation involve 25–26 species. The quasi-global model therefore occupies an intermediate position between the simplest and most detailed models, in terms of computer time requirements.

The rate parameters for fuel consumption in the quasi-global model depend on the type of application being studied (Edelman and Fortune). Different pre-exponential terms must be used for flow systems and for stirred reactors. We found this to be true as well for applications to flames. The fuel consumption reaction is written to produce CO and H_2. For example, for n-paraffin fuels

$$C_nH_{2m} + \frac{n}{2}O_2 = nCO + mH_2. \qquad (12)$$

This was combined with 21 elementary reactions involving the H_2–O_2–CO mechanism. The global reaction rate for Reaction 12 was determined for each type of fuel as described earlier and the best rate parameters are summarized in Table IV. The reactions and rate parameters used for the H_2–O_2–CO mechanism are given in Table V. The computed flame speeds as functions of equivalence ratio and pressure are essentially indistinguishable from those found from the single-step and two-step mechanisms discussed earlier. The principal advantage is the further improvement in the burned gas composition and temperature, although the flame structure and species concentrations in the flame zone cannot presently be predicted well by the quasi-global mechanism.

TABLE V

Reaction mechanism used in quasi-global mechanism for CO–H_2–O_2 system. Reverse rates computed from relevant equilibrium constants. Same units as Table I

Reaction	A	n	E_a
$H+O_2=O+OH$	2.2×10^{14}	0.0	16.8
$H_2+O=H+OH$	1.8×10^{10}	1.0	8.9
$O+H_2O=OH+OH$	6.8×10^{13}	0.0	18.4
$OH+H_2=H+H_2O$	2.2×10^{13}	0.0	5.1
$H+O_2+M=HO_2+M$	1.5×10^{15}	0.0	−1.0
$O+HO_2=O_2+OH$	5.0×10^{13}	0.0	1.0
$H+HO_2=OH+OH$	2.5×10^{14}	0.0	1.9
$H+HO_2=H_2+O_2$	2.5×10^{13}	0.0	0.7
$OH+HO_2=H_2O+O_2$	5.0×10^{13}	0.0	1.0
$HO_2+HO_2=H_2O_2+O_2$	1.0×10^{13}	0.0	1.0
H_2O_2+M $=OH+OH+M$	1.2×10^{17}	0.0	45.5
$HO_2+H_2=H_2O_2+H$	7.3×10^{11}	0.0	18.7
$H_2O_2+OH=H_2O+HO_2$	1.0×10^{13}	0.0	1.8
$CO+OH=CO_2+H$	1.5×10^{7}	1.3	−0.8
$CO+O_2=CO_2+O$	3.1×10^{11}	0.0	37.6
$CO+O+M=CO_2+M$	5.9×10^{15}	0.0	4.1
$CO+HO_2=CO_2+OH$	1.5×10^{14}	0.0	23.7
$OH+M=O+H+M$	8.0×10^{19}	−1.0	103.7
$O_2+M=O+O+M$	5.1×10^{15}	0.0	115.0
$H_2+M=H+H+M$	2.2×10^{14}	0.0	96.0
$H_2O+M=H+OH+M$	2.2×10^{16}	0.0	105.0

Both the strengths and weaknesses of the quasi-global approach can be illustrated by comparing species and temperature profiles computed with a quasi-global reaction mechanism with those computed with a full detailed mechanism. This was done for the case of a stoichiometric methanol–air mixture at atmospheric pressure, using a detailed mechanism taken from our previous study (Westbrook and Dryer, 1980a). Both models correctly reproduced the observed laminar flame speed of 44 cm/sec. Computed results are summarized in Figures 3 and 4. The temperature and fuel concen-

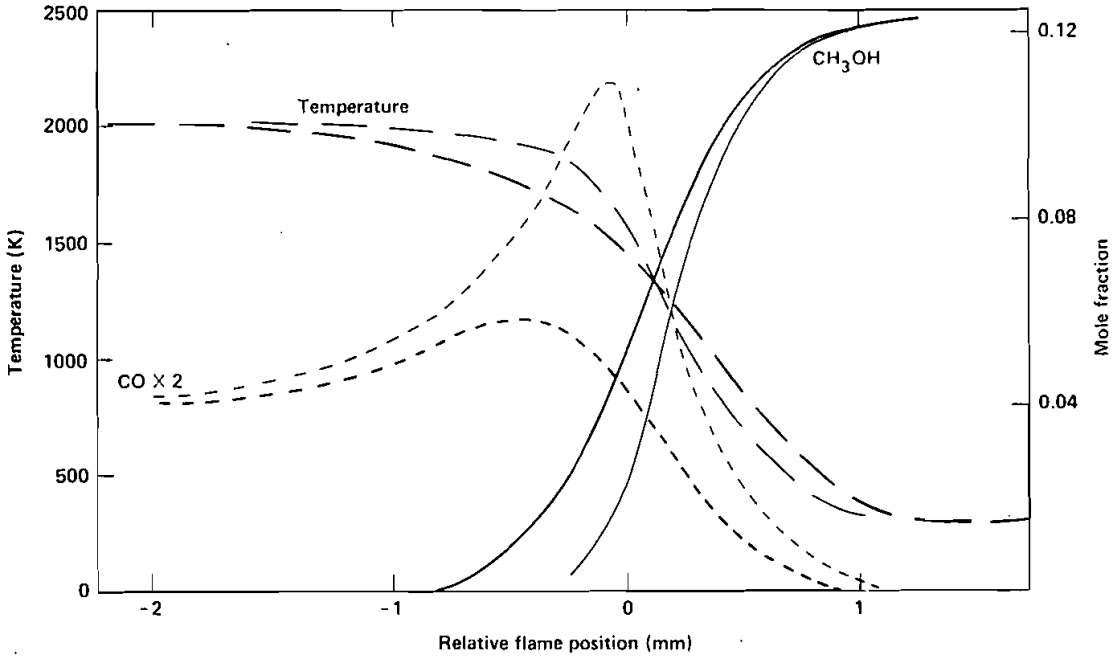

FIGURE 3 Temperature, methanol, and carbon monoxide concentrations in a stoichiometric methanol–air flame at atmospheric pressure, computed using detailed reaction mechanism (light curves) and quasi-global mechanism (heavy curves), all as functions of relative flame position.

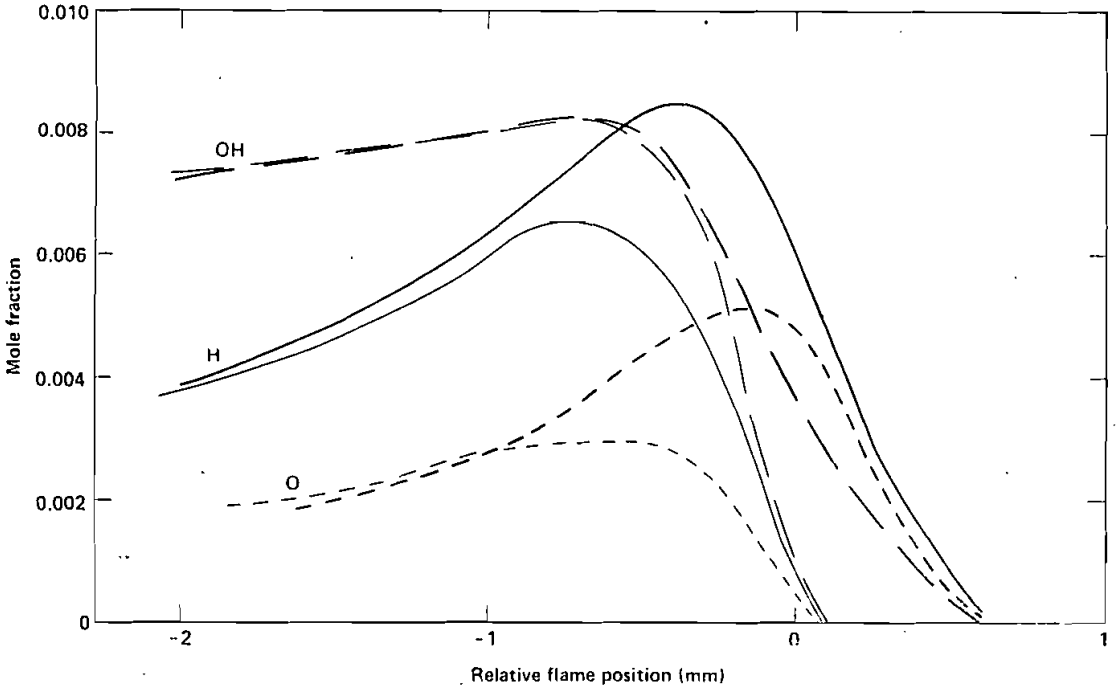

FIGURE 4 Concentration profiles for H, O, and OH radicals as functions of relative flame position for the same flame models as in Figure 3.

tration profiles are in fairly good agreement, with the detailed model predicting a slightly steeper rate of fuel consumption and temperature increase in the flame region ($1200 \leqslant T \leqslant 1800$ K). Similar agreement was observed for computed O_2, CO_2, and H_2O profiles. There is a substantial qualitative difference, however, between the computed CO profiles. The detailed model predicts a much higher CO concentration in the pre-flame and flame regions ($-0.05 \leqslant x \leqslant 0.10$ cm), although both models predict the same equilibrium CO level in the post-flame region. Related trends can be seen for radical species H, O, and OH in Figure 4. Here the quasi-global mechanism predicts substantially larger concentrations of H and O in the flame and pre-flame regions, with closer agreement between the two computed OH profiles. Perhaps the most distinctive feature is that the concentrations of all three radical species fall sharply below 100 ppm at different positions, near $x = 0.0$ cm in the detailed models and at $x = 0.06$ cm in the quasi-global model.

We have discussed the reasons for these differences previously (Dryer and Westbrook), showing how the simplified mechanism predicts incorrect radical species concentrations in regions which contain unreacted fuel and other hydrocarbon species. Reaction rates between radical species such as O, H, and OH and hydrocarbon molecules such as CH_3OH, CH_4, C_2H_6, and others are generally much greater than between the same radical species and CO or H_2. Therefore, when fuel or other hydrocarbon species still remain, the radicals cannot react with CO or H_2. Radical species levels are kept very small until the hydrocarbons are consumed, whereupon CO and H_2 oxidation can begin, as illustrated for CO in Figure 3. However, the quasi-global mechanism does not explicitly consider reactions between radical species and fuel molecules, using an overall rate expression like that of Eq. (7). As a result, there is no means of keeping the radical concentrations low in regions in which fuel remains. This can easily be seen in Figure 4 where the H, O, and OH levels in the range ($-0.06 \leqslant x \leqslant +0.05$ cm) computed by the quasi-global model are greater than 1000 ppm even though the CH_3OH concentration in that range remains above 1 percent. Because the radical species are so high in this region of the quasi-global model, CO oxidation begins sooner than in the detailed model. Therefore the CO concentration computed by the quasi-global model remains substantially lower than in the detailed model in which the presence of the fuel effectively inhibits CO oxidation.

DISCUSSION

The procedures described here can be applied to any type of fuel molecule to develop and validate simplified reaction mechanisms. We have illustrated the basic method with some hydrocarbon fuels of common interest, but other fuels, including non-hydrocarbons, can be treated in the same way. As an example, flame speeds for methyl-substituted *n*-paraffins are several centimeters per second smaller than for straight-chain molecules of the same overall composition and their flammability limits are slightly narrower (Dugger *et al.*). Thus the flame speed at atmospheric pressure for a stoichiometric mixture of isooctane (2,2,4-trimethyl pentane) in air is about 36 cm/sec while that for *n*-octane is about 40 cm/sec. The rich flammability limit for isooctane is $\phi_R' = 3.6$ and about 4.25 for *n*-octane. If the rate parameters for *n*-octane in Table I are used, but the pre-exponential A is multiplied by 0.81 (*i.e.* $(36/40)^2$), then the single-step reaction mechanism reproduces the experimental data well for isooctane. This scaling of the pre-exponential can be done for many of the methyl-substituted paraffin fuels.

For each set of reaction rate parameters, the pre-exponential terms tabulated here should be regarded as approximate values if they are used in other numerical models. In addition to rate parameters, flame speeds depend on thermodynamic and transport properties which may be treated somewhat differently in other models. The activation energies and concentration exponents derived here should be valid for other models. Therefore, for use in other codes, the parameters presented here should be used as initial estimates, with comparisons between computed and experimental data for some reference condition serving to calibrate the pre-exponential factor A.

The most significant result of the modeling work discussed in this paper is the development of a systematic, direct means of determining rate parameters for global reactions which can be used to model flame propagation. In contrast with other simplified reaction rate expressions in common use, the rates derived in this manner correctly reproduce experimental flame speeds over wide ranges of equivalence ratio and pressure. This avoids the problem demonstrated for rate expressions which assume that the fuel consumption reaction is first order in fuel and oxidizer concentrations. With those parameters flame speeds and flammability limits for fuel-rich mixtures are seriously overestimated.

All of the simplified mechanisms from Tables I and IV predicted laminar flame speeds equally well, including variations with equivalence ratio and pressure. The addition of intermediate species such as CO, H_2, and others together with further refinement of the reaction mechanism into several steps makes the predicted product temperature and composition more accurate, at the expense of requiring more computer time. The particular needs of each model application must determine the appropriate level of simplification.

Extension of these results to turbulent regimes is a complex problem involving many currently unanswered questions. However, some numerical models which treat heat and species transport in turbulent regimes by means of eddy diffusivities (*e.g.* Butler *et al.*, 1980; Gupta *et al.*, 1980) have had considerable success in simulating turbulent combustion in internal combustion engines using single-step global reaction rates like Eq. (2). In such models the conclusions regarding fuel and oxygen concentration exponents reached here for laminar conditions will apply, and the use of rate expressions which are first order in fuel and oxidizer concentrations should be avoided.

ACKNOWLEDGEMENT

We acknowledge with pleasure valuable discussions with Professor Forman Williams. This work was performed in part under the auspices of the U.S. Department of Energy by the Lawrence Livermore National Laboratory under contract number W-7405-ENG-48.

REFERENCES

Adamczyk, A. A., and Lavoie, G. A. (1978). Laminar head-on flame quenching—a theoretical study. *SAE Transactions*, Vol. 87, SAE paper 780969.

Andrews, G. E., and Bradley, D. (1972). The burning velocity of methane-air mixtures. *Combustion and Flame*, **19**, 175.

Bowman, C. T. (1970). An experimental and analytical investigation of the high temperature oxidation mechanisms of hydrocarbon fuels. *Combustion Science and Technology*, **2**, 161.

Butler, T. D., Cloutman, L. D., Dukowicz, J. K., Ramshaw, J. D., and Krieger, R. B. (1980). Toward a comprehensive model for combustion in a direct-injection stratified-charge engine. In Mattavi, J. N., and Amann, C. A. (Eds.). *Combustion Modeling in Reciprocating Engines*, Plenum, New York, pp. 231–264.

Dryer, F. L., and Glassman, I. (1972). High-temperature oxidation of CO and CH_4. *Fourteenth Symposium (International) on Combustion*, The Combustion Institute, Pittsburgh, p. 987.

Dryer, F. L., and Westbrook, C. K. (1979). Chemical kinetic modelling for combustion applications. Paper presented at the Propulsion and Energetics Panel 54th Specialist's Meeting, Cologne, West Germany, October 1979. NATO AGARD Conference Proceedings No. 275, University of California, Lawrence Livermore National Laboratory report UCRL-81777, September 1979.

Dugger, G. L., Simon, D. M., and Gerstein, M. (1959). Laminar flame propagation. Chapter IV in N.A.C.A. Report #01300.

Edelman, R. B., and Fortune, O. F. (1969). A quasi-global chemical kinetic model for the finite rate combustion of hydrocarbon fuels with application to turbulent burning and mixing in hypersonic engines and nozzles. AIAA paper 69-86.

Fenn, J. B., and Calcote, H. F. (1952). Activation energies in high temperature combustion. *Fourth Symposium (International) on Combustion*, Williams and Wilkins, Baltimore, pp. 231–239.

Garforth, A. M., and Rallis, C. J. (1978). Laminar burning velocity of stoichiometric methane-air: pressure and temperature dependence. *Combustion and Flame*, **31**, 53.

Gupta, H. C., Steinberger, R. L., and Bracco, F. V. (1980). Combustion in a divided chamber, stratified charge, reciprocating engine: Initial comparisons of calculated and measured flame propagation, *Combustion Science and Technology*, **22**, 27–62.

Heffington, W. M., Parks, G. E., Sulzmann, K. G. P., and Penner, S. S. (1976). Studies of methane oxidation kinetics. *Sixteenth Symposium (International) on Combustion*, The Combustion Institute, Pittsburgh, pp. 997–1011.

Lewis, B., and von Elbe, G. (1961). *Combustion, Flames and Explosions of Gases*. Academic Press, New York.

Lund, C. M. (1978). HCT-A general computer program for calculating time-dependent phenomena involving one-dimensional hydrodynamics, transport, and detailed chemical kinetics. University of California Lawrence Livermore National Laboratory Report UCRL-52504.

Metghalchi, M., and Keck, J. C. (1977). Laminar burning velocity of isooctane-air, methane-air, and methanol-air mixtures at high temperature and pressure. Paper presented at the Fall Meeting of the Eastern Section of The Combustion Institute, Hartford, Connecticut.

Metghalchi, M., and Keck, J. C. (1980). Laminar burning velocity of propane-air mixtures at high temperature. *Combustion and Flame*, **38**, 143.

Semenov, N. N. (1942). Thermal theory of combustion and explosion. III—Theory of normal flame propagation. N.A.C.A. Report 1026.

Simon, D. M. (1951). Flame propagation. III. Theoretical consideration of the burning velocities of hydrocarbons. *J. Am. Chem. Soc.*, **73**, 422.

Smoot, L. D., Hecker, W. C., and Williams, G. A. (1976). Prediction of propagating methane-air flames. *Combustion and Flame*, **26**, 323.

Tsatsaronis, G. (1978). Prediction of propagating laminar flames in methane, oxygen, nitrogen mixtures. *Combustion and Flame*, **33**, 217.

Walker, P. L., and Wright, C. C. (1952). Hydrocarbon burning velocities predicted by thermal versus diffusional mechanisms. *J. Am. Chem. Soc.*, **74**, 3769.

Westbrook, C. K. (1979). An analytical study of the shock tube ignition of mixures of methane and ethane. *Combustion Science and Technology*, **20**, 5.

Westbrook, C. K., and Dryer, F. L. (1979). A comprehensive mechanism for the oxidation of methanol. *Combustion Science and Technology*, **20**, 125.

Westbrook, C. K., and Dryer, F. L. (1980a). Prediction of laminar flame properties of methanol-air mixtures. *Combustion and Flame*, **37**, 171.

Westbrook, C. K., and Dryer, F. L. (1980b). Chemical kinetics and modeling of combustion processes. *Eighteenth Symposium (International) on Combustion*, The Combustion Institute, Pittsburgh, p. 749.

Zeldovich, Y. B., and Frank-Kamenetsky, D. A. (1938). *J. Phys. Chem. Moscow*, **12**, 100.